

## Supporting Information

### Emergence of practical fluorescence in a confined space of nanoporous silica: significantly enhanced quantum yields of a conjugated molecule

Kosei Hayashi,<sup>\*a,b</sup> Yasuto Fujimaki,<sup>a</sup> Kentaro Mishiba,<sup>a</sup> Hiroto Watanabe,<sup>b</sup> and Hiroaki Imai<sup>b</sup>

<sup>a</sup>*Tokyo Metropolitan Industrial Technology Research Institute, 2-4-10 Aomi, Koto-ku, Tokyo 135-0064, Japan. E-mail: hayashi.kosei@iri-tokyo.jp*

<sup>b</sup>*Department of Applied Chemistry, Faculty of Science and Technology, Keio University, 3-14-1 Hiyoshi, Kohoku-ku, Yokohama 223-8522, Japan.*

#### Experimental

We prepared supermicroporous silicas (SMPSs) and mesoporous silicas (MPSs) by the solvent-free process as shown in Fig. S1. Alkyl trimethylammonium chloride (bromide) ( $C_n$ TAC(B),  $n$ : carbon number of alkyl chain ( $n = 6-18$ )), tetraethyl orthosilicate (TEOS), and water acidified with HCl (pH 2.0) were mixed in a molar ratio of 0.2:1.0:4.0. In the present study,  $N,N,N$ -trimethylhexylammonium bromide ( $C_6$ TAB) and trimethylstearyl ammonium chloride ( $C_{18}$ TAC) were used as a surfactant and a template for an SMPS and an MPS, respectively. After the mixture was stirred at 298 K until gelation, the products were dried at 333 K for 24 h and calcined at 873 K for 3 h in air. The detailed synthesis procedures and the characterization of porous silicas were described in our previous reports.<sup>1</sup> Crushed monolith of the SMPS and MPS were used for this research

Porous silicas with pore diameters from  $\sim 1$  to 3 nm, and silica nanoparticles (Tokuyama Reolosil<sup>TM</sup>, diameter: ca. 20 nm, specific surface area: ca. 210 m<sup>2</sup>/g, the average size of interparticle pores, 11 nm) were soaked in a methanol solution saturated with benzanthrone (BA) (1 mmol/dm<sup>3</sup>) for 24 h. The outer surface of the SMPS and MPS was washed with a small amount of methanol and then dried under vacuum for 24 h to remove the solvents.

The pore structure in porous silicas was characterized by nitrogen adsorption isotherms obtained at 77 K (BEL Japan Inc., BELSORP-max) using samples preheated under vacuum at 433 K for 5 h. The specific surface area was calculated using the Brunauer-Emmett-Teller (BET) method. The average pore diameter in the micropore region was calculated by the grand canonical Monte Carlo (GCMC) method using BEL-Master<sup>TM</sup> ver. 6.4.10 software assuming an oxygen-exposed surface with a cylindrical pore structure. IR spectra of porous silica were measured by JASCO FT-IR 4300 and IRT-5000. Absolute photoluminescence, quantum yield (QY), and fluorescence spectra were measured by a Hamamatsu Photonics C9920-02G. The QY was calculated by the ratio of the number of photons absorbed by the sample to the number of photons emitted. The number of photons absorbed by the sample was measured from the difference between the excitation spectrum of the empty quartz glass

cell and the excitation spectrum of the quartz glass cell containing the sample. The number of photons emitted by the luminescence was measured from the luminescence spectrum of the sample. The molecule of BA incorporating into the SMPSs pore was analyzed by nitrogen adsorption isotherms obtained at 77 K (BEL Japan Inc., BELSORP-max) using samples preheated under vacuum at 393 K for 4 h. In addition, the molecules of BA incorporating into the SMPSs and MPSs pore was measured by thermogravimetric differential thermal analysis (TG-DTA) by a Shimadzu DTG-60 in air. The molecules of BA incorporating in the SMPSs pores, in solid state, and on the surface of silica nanoparticles were analyzed by Raman spectroscopy (Renishaw InVia Reflex) with a laser beam of 785 nm in wavelength.

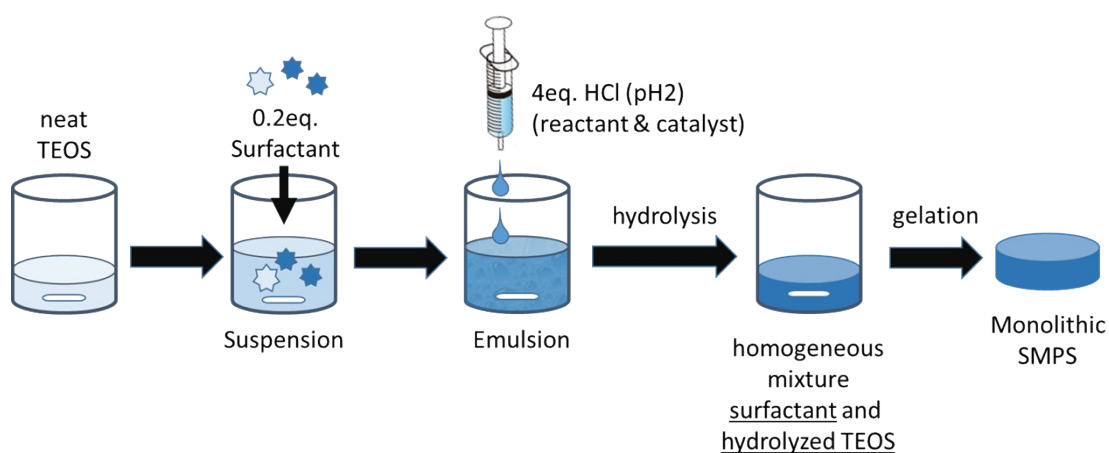


Figure S1. A schematic illustration of the solvent-free process for synthesis of porous silicas. Crushed monolith of the SMPS and MPS were used for this research.

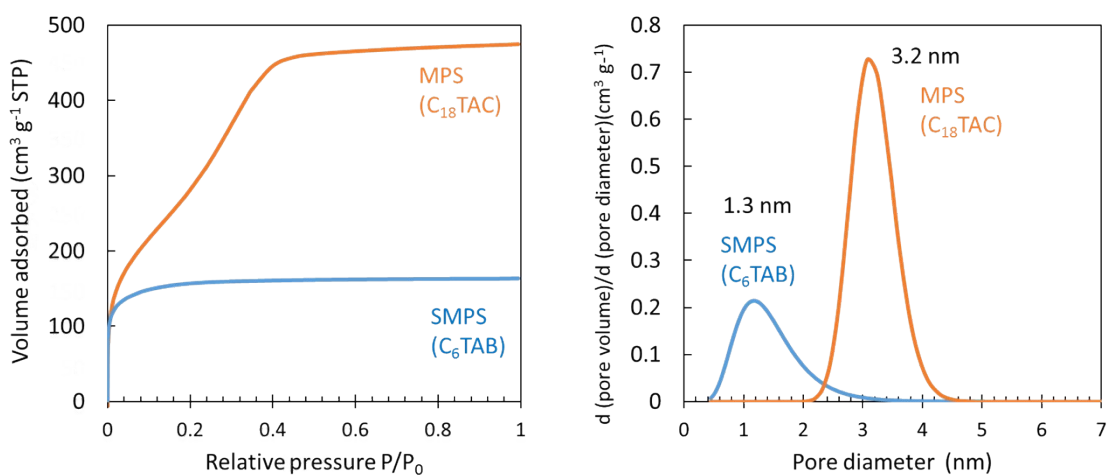


Figure S2. Nitrogen adsorption isotherms (left) and pore-size distribution estimated by the GCMC method (right) for the SMPS and MPS prepared with C<sub>6</sub>TAB and C<sub>18</sub>TAC, respectively.

Table S1. Properties of MPS and SMPS.

Sample	SSA <sup>(a)</sup>		TPV <sup>(b)</sup>	
	BET		BJH <sup>(c)</sup>	GCMC <sup>(d)</sup>
	m <sup>2</sup> /g	cm <sup>3</sup> /g	nm	nm
C18 MPS	1491	0.77	2.44	3.22
C6 SMPS	572	0.27	-	1.21

(a) Specific surface area calculated from BET method. (b) Total pore volume. (c), (d) (e) Calculated average pore diameters using BJH and GCMC analysis.

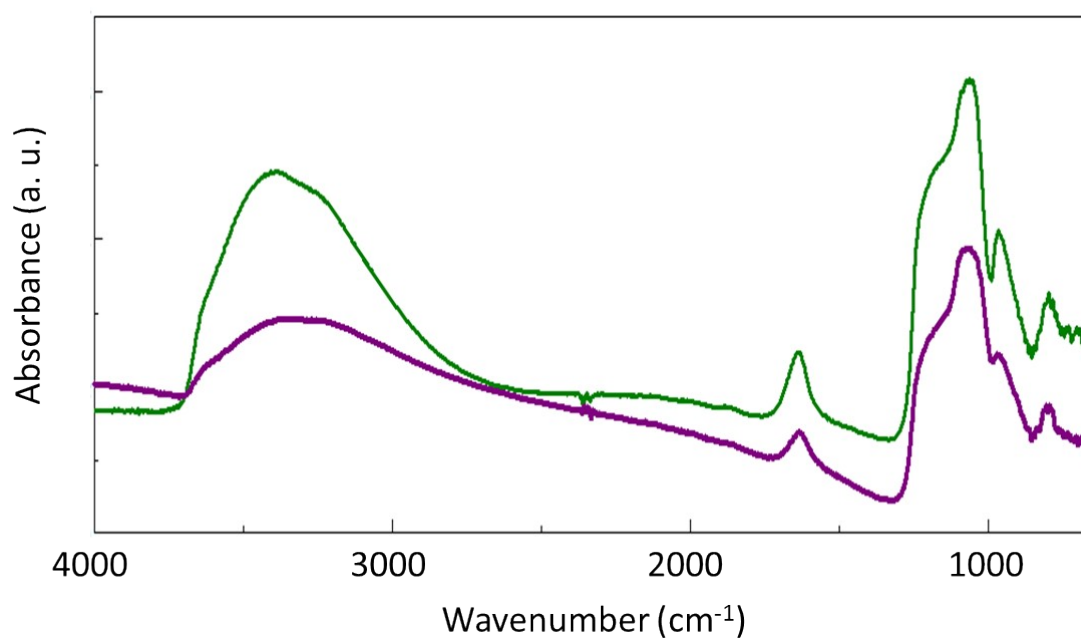


Figure S3. IR spectra of C6 SMPS (green line) and C18 MPS (purple line).

Table S2. Total pore volume of the porous materials estimated by BET experiment. (measured by nitrogen adsorption isotherms)

State	Total pore volume (cm <sup>3</sup> /g)
C6 SMPS	0.27
BA incorporating into the C6 SMPSs pores	0.25
C18 MPS	0.69

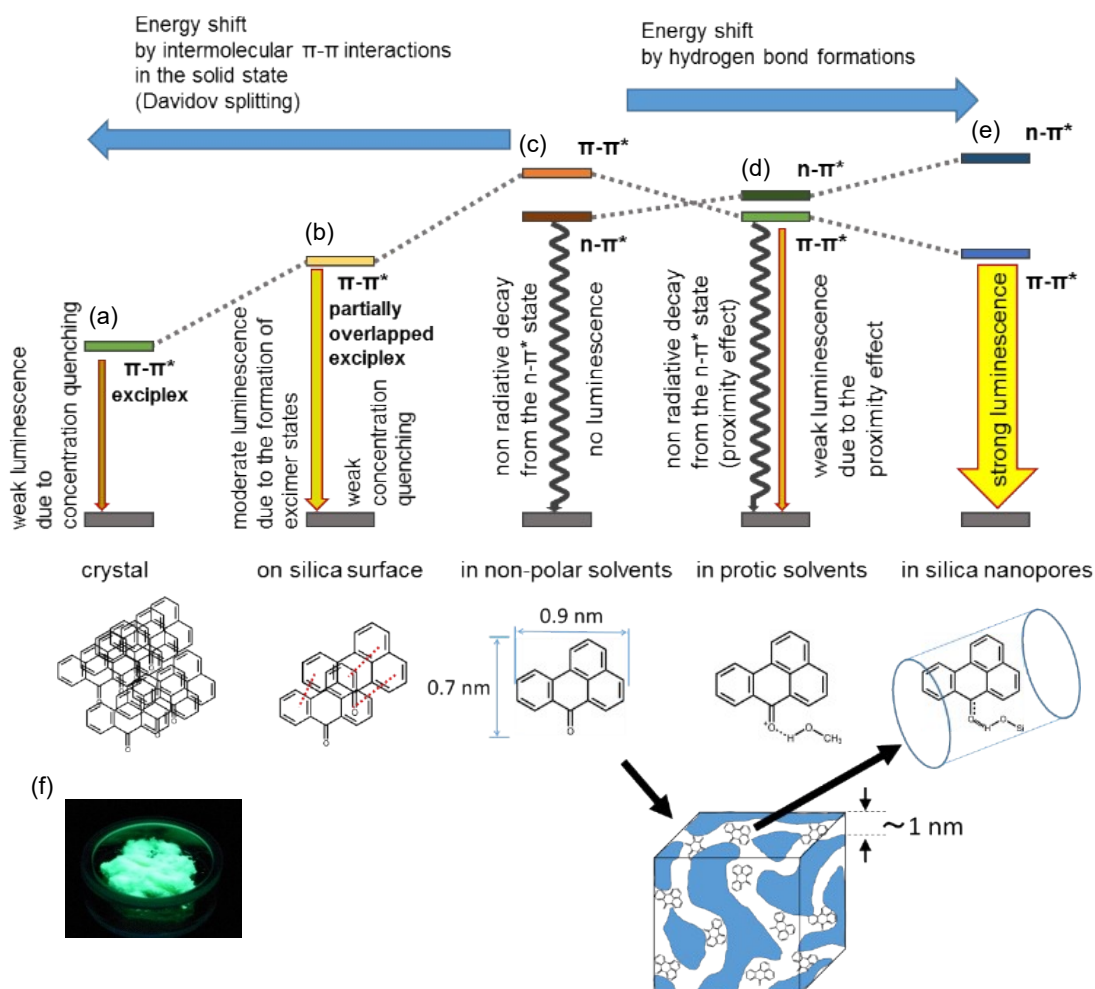


Fig. S4 Schematic illustration of energy states and molecular structures of BA crystal (solid state) (a), on the silica surface (b), in a nonpolar solvent (c), in a protic solvent (d), and in nanopores of silica (d). Photograph of the fluorescence of BA under UV light (365 nm) in a solid state (f).

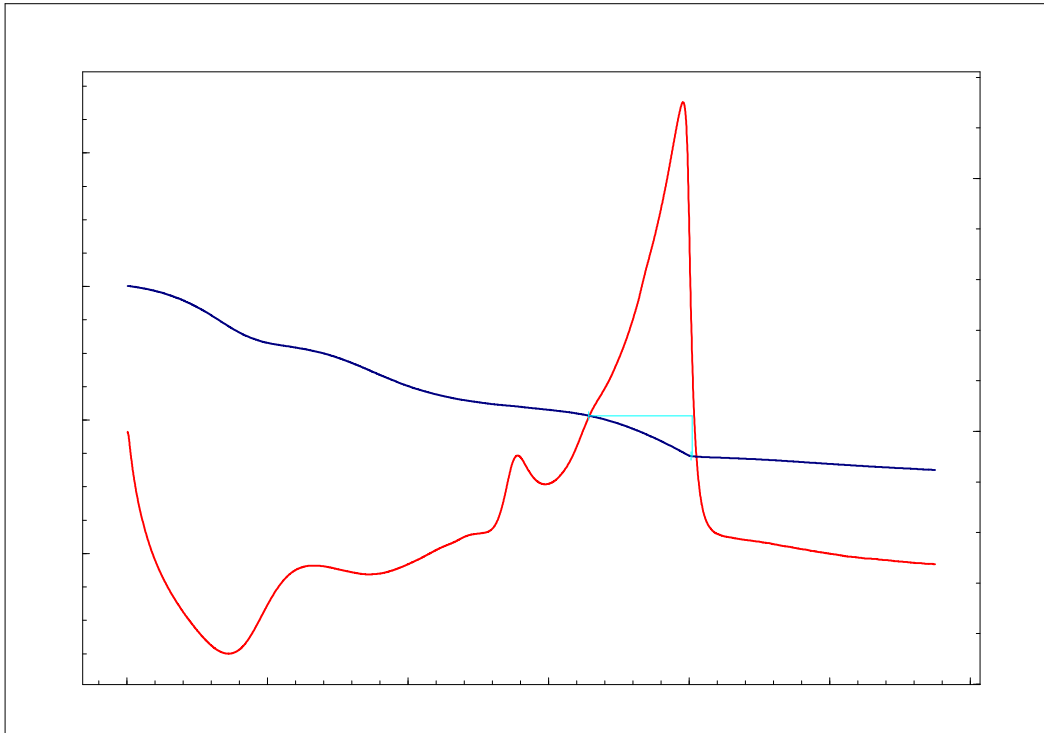


Figure S5. TG-DTA curve of BA incorporated into the pore of SMPSs.

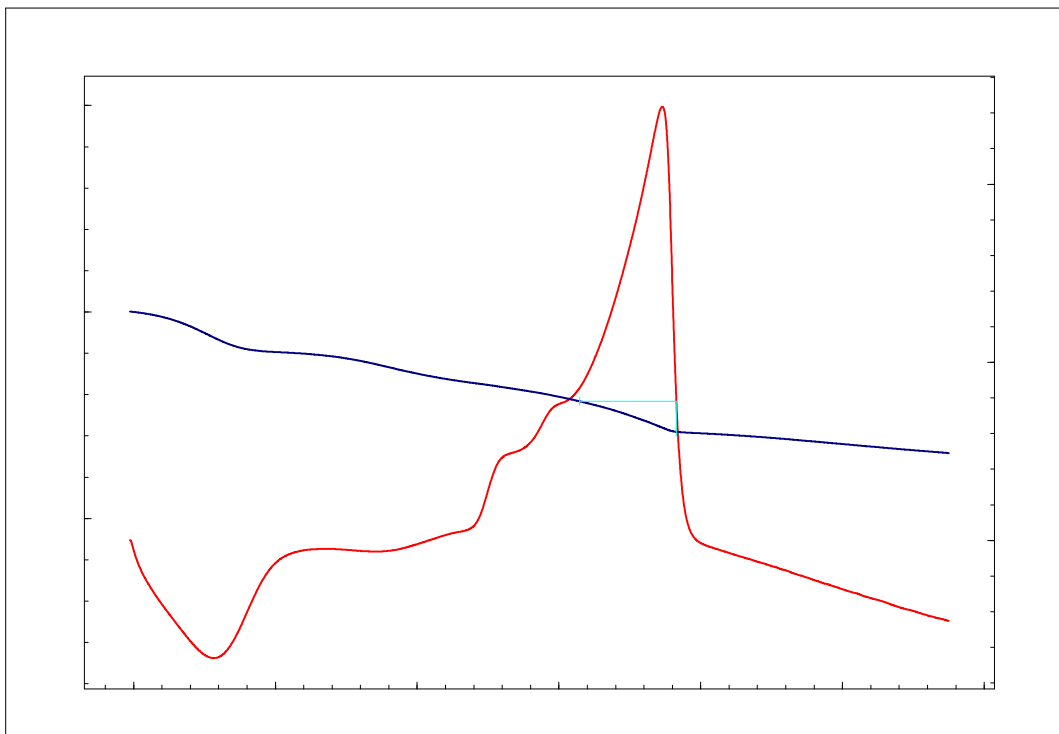


Figure S6. TG-DTA curve of BA incorporated into the pore of MPSs.

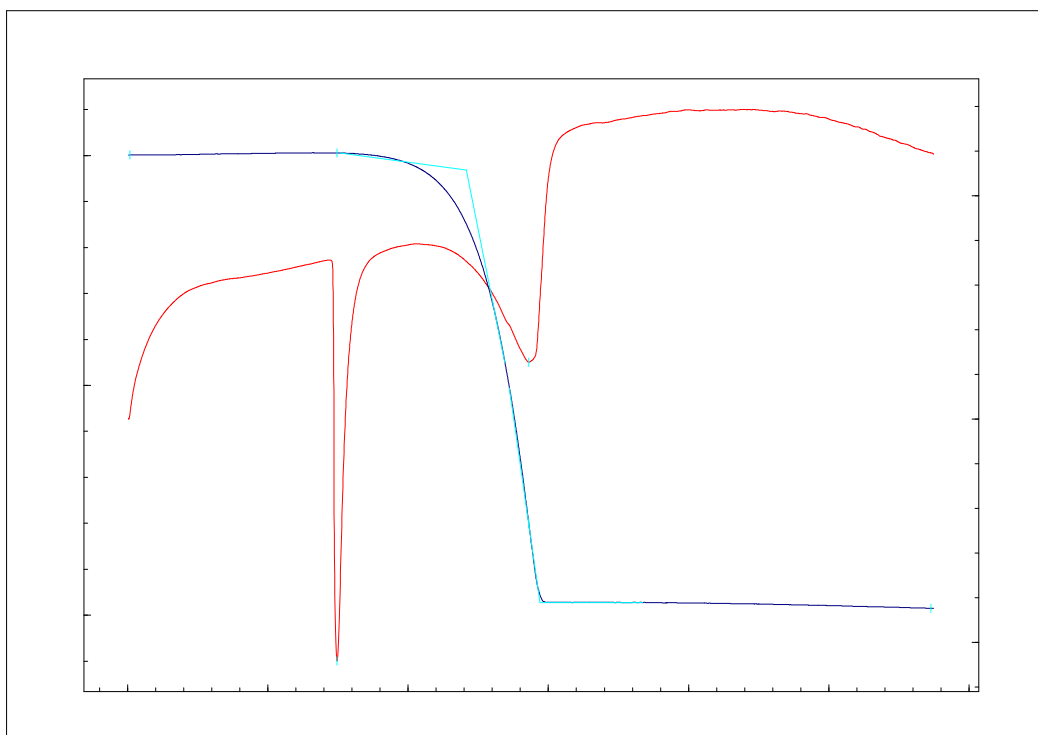


Figure S7. TG-DTA curve of BA. (solid state)

Table S3. Quantum yields of BA in various states.

State	Quantum yields
in pores (1.3 nm)	0.62
in pores (3.2 nm)	0.42
on the silica surface	0.28
in Wakogel 50C18 (for reverse phase chromatography, without Si-OH)	0.16
solid state	0.05
in MeOH (protic solvent)	0.03
in nonpolar and aprotic solvents <sup>(a)</sup>	< 0.01

(a) Nonpolar solvents and aprotic solvents are benzene, chloroform, carbon tetrachloride, hexane, toluene, acetone, ethyl acetate and tetrahydrofuran.

Table S4. The wavelength, oscillator strength, and assignment of absorption bands of BA in the UV region calculated by the TDDFT (B3LYP / 6-31g (d) levels) method.

$\lambda/\text{cm}^{-1}$ (nm)	Oscillator strength ( $f$ )	Major contributions	Major assignment
25063 (399)	0.0000	HOMO-1 $\rightarrow$ LUMO	$n-\pi^*$
25510 (392)	0.1865	HOMO $\rightarrow$ LUMO	$\pi-\pi^*$

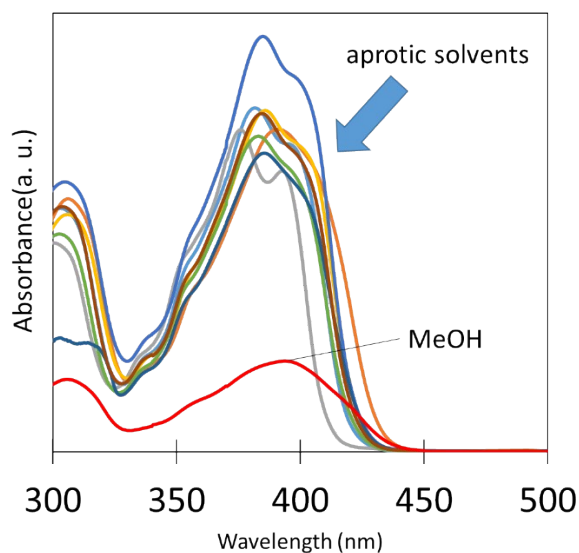


Figure S8. The UV-vis absorption spectra for BA in a protic solvent (red line: methanol) and aprotic solvents (another lines:  $\text{CCl}_4$ ,  $\text{CHCl}_3$ , hexane, benzene, toluene, ethyl acetate, acetone and THF).

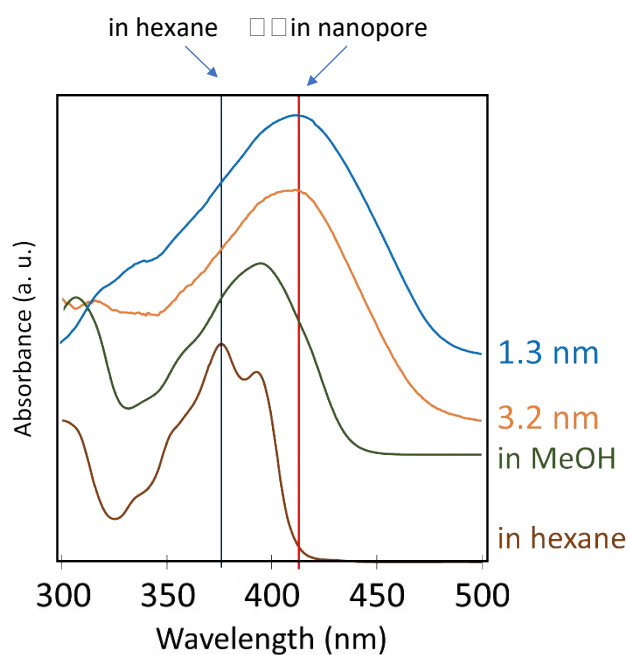


Figure S9. UV-vis spectra of BA in aprotic solvents (brown: hexane), in a protic solvent (green:

methanol), in the 3.2 nm pore (orange), and in the 1.3 nm pore (blue). Spectra were obtained by the transmission method for the solutions containing 0.05 mmol/dm<sup>3</sup> BA and by the diffuse reflectance method for BA incorporated in the pores of porous silicas.

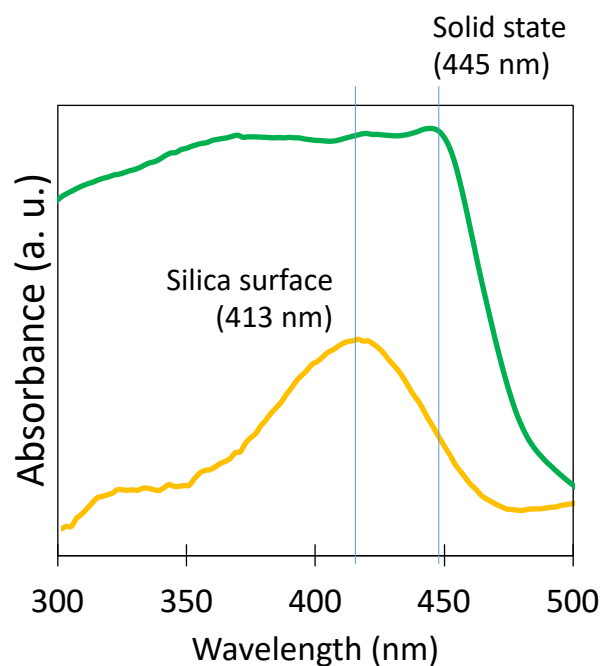


Figure S10. The UV-vis absorption spectra for BA in the solid state and on the surface of silica nanoparticles.

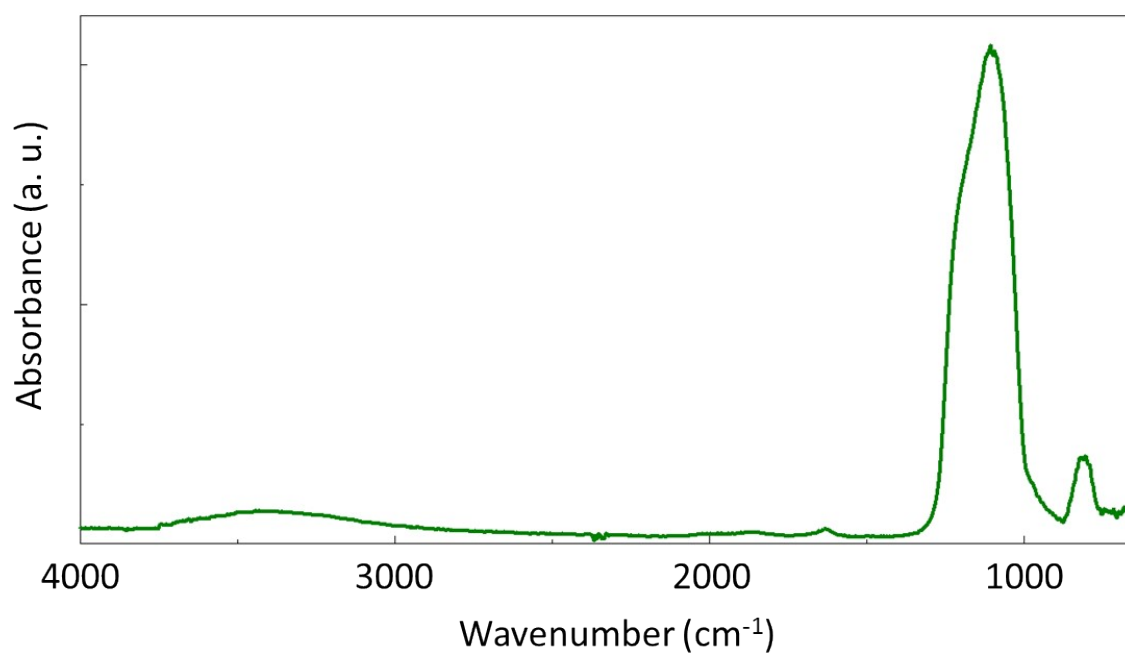




Figure S11. IR spectrum of silica nanoparticles.

**Reference**

1. H. Watanabe, K. Fujikata, Y. Oaki, H. Imai, *Microporous Mesoporous Mater.* 2015, **214**, 41.